https://doi.org/10.5194/egusphere-2024-2982
Preprint. Discussion started: 30 October 2024

Approximating ice sheet – bedrock interaction in Antarctic ice sheet projections

Caroline J. van Calcar[1,2], Pippa L. Whitehouse[3], Roderik S.W. van de Wal[1,4] & Wouter van der Wal[2]
[1]Institute for Marine and Atmospheric research Utrecht, Utrecht University, Utrecht, 3508 TA, The Netherlands
[2]Faculty of Aerospace Engineering, Delft University of Technology, Delft, 2629 HS, The Netherlands
[3]Department of Geography, Durham University, Durham, UK
[4]Department of Physical Geography, Utrecht University, Utrecht, 3584 CB, The Netherlands

Correspondence to: Caroline J. van Calcar (c.j.vancalcar@uu.nl)

Abstract. The bedrock response to a melting ice sheet provides a negative feedback on ice mass loss. When modelling the future behaviour of the Antarctic Ice Sheet, accounting for the impact of bed deformation on ice dynamics can reduce predictions of future sea level rise by up to 40% in comparison with scenarios that assume a rigid Earth. The rate of the solid Earth response is mainly dependent on the viscosity of the Earth's mantle, which varies laterally and radially with several orders of magnitude across Antarctica. Because modelling the response for a varying viscosity is complex, sea level projections often exclude the Earth's response, or apply a globally constant relaxation time or viscosity. We investigate how accurate such approximations are using an ice sheet model coupled with a glacial isostatic adjustment (GIA) model that simulates the bedrock response to changes in ice loading including lateral and radial variations in viscosity (3D GIA model). Using the 3D model we determined a relation between relaxation time and viscosity which can be used in simpler models. We compare output from an elastic lithosphere relaxed asthenosphere (ELRA) with uniform and laterally varying relaxation times, and a GIA model with a radially varying Earth structure (1D GIA model) and a 3D GIA model. We conducted 500 year projections of the Antarctic ice sheet evolution using two different climate models and two emissions scenarios: the high emission scenario SSP5-8.5 and the low emission scenario SSP1-2.6. The results show that using a uniform relaxation time of 300 years in the ELRA model or an upper mantle viscosity of 10^{19} Pa·s in the 1D GIA model leads to a total sea level rise that deviates less than 40 cm from the average of the 3D GIA models. This difference in the sea level rise predicted with 1D and 3D GIA models can be further reduced to 10 cm by using laterally varying relaxation time maps in an ELRA model. Our results show that the effect of 3D viscosity variations on the AIS contribution to sea level rise can be approximated using the ELRA model or a 1D GIA model when the recommended parameters derived from the full 3D GIA model are used.

1 Introduction

The Antarctic ice sheet might contribute several meters to global mean sea level rise over the next centuries (Fox-Kemper et al., 2021). The rate of ice loss is influenced by many processes such as atmospheric and oceanic feedbacks, ice dynamics, and interactions with the underlying bedrock. Accurately representing these processes in models, along with their associated

https://doi.org/10.5194/egusphere-2024-2982
Preprint. Discussion started: 30 October 2024

uncertainties, presents a significant challenge for projecting the ice sheet evolution. To address this, a wide range of parameters in the ice sheet model must be explored, requiring thousands of simulations to produce robust projections of potential sea level rise over the coming centuries (Seroussi et al., 2020).

One of the main uncertainties in projecting the evolution of the Antarctic ice sheet over the next centuries is the response of the solid Earth to future changes in ice mass (Fox-Kemper et al., 2021). The bedrock experiences uplift due to the loss of ice mass at the surface, a process known as glacial isostatic adjustment (GIA). The bedrock uplift can delay grounding line retreat and thereby stabilize the ice sheet (Konrad et al., 2015; Pollard et al., 2017; Whitehouse et al., 2019; Kachuck et al., 2020; Coulon et al., 2021; Book et al., 2022; Gomez et al., 2024; van Calcar et al., 2024). The rate of the bedrock uplift depends on the viscosity of the Earth's mantle, which varies both radially and laterally by several orders of magnitude beneath the Antarctic ice sheet (Kaufmann et al., 2005; Ivins et al., 2023), as derived from seismic models (e.g. Lloyd et al., 2019). Therefore, bedrock uplift is influenced not only by the amount of ice mass loss but also by the specific region where the loss occurs. Models that include the solid Earth feedback for a realistic Earth structure project a maximum of 23-40% reduction in sea level rise over the coming centuries compared with models that assume a rigid Earth (Gomez et al., 2024; van Calcar et al., 2024), and a delay in grounding line retreat in the Amundsen Sea Embayment by up to 130 years (van Calcar et al., 2024). However, it is currently unfeasible to include a realistic Earth structure in a large ensemble of sea level projections due to the long computation time involved (van Calcar et al., 2023). Therefore, projections of the Antarctic ice sheet evolution by ice sheet models either omit bedrock uplift or use simplified Earth models (Levermann et al., 2020).

One such simplified model that is commonly coupled to ice sheet models is the elastic lithosphere relaxed asthenosphere (ELRA) model. ELRA models are computationally cheap and can be used in combination with a range of ice models, allowing large ensembles of sea level projections to be simulated (Bulthuis et al., 2019; DeConto et al., 2021; Coulon et al., 2024). Typically, the ELRA model is used with a uniform relaxation time of 3000 years and a flexural rigidity of 10^{25} kg m^2 s^{-2}, which roughly corresponds to a lithospheric thickness of 100 km. The relaxation time of the Earth's mantle, which is a characteristic time scale that expresses how fast the mantle responds to changes in surface loads, serves as a proxy for mantle viscosity because it also reflects how fast the viscous mantle flows under stress. Flexural rigidity is the resistance of a body, such as the Earth's lithosphere, to bending and is determined, among other, by its stiffness (the elastic modulus) and its thickness.

Alternatively, some sea level projections use ice sheet models coupled with a 1D GIA model. A GIA model can include the bedrock response to changes in ice loading, and can additionally solve the sea level equation to include changes in ocean loading. In this study, we use the term GIA model for a model that computes deformation based on ice loading only. A 1D GIA model includes an Earth structure where viscosity varies radially and not laterally, equivalent to a self gravitating viscoelastic Earth (SGVE) model (Le Meur and Huybrechts, 1996). Current existing ice sheet projections use a homogeneous upper mantle viscosity of 10^{21} Pa·s (Gomez et al., 2015; Konrad et al., 2015; Rodehacke et al., 2020; Golledge et al., 2019). However, using such a viscosity value, or a relaxation time of 3000 years, does not affect sea level rise projections significantly compared with excluding GIA entirely, and it overestimates sea level rise by up to 20% by the year 2500 compared with

https://doi.org/10.5194/egusphere-2024-2982
Preprint. Discussion started: 30 October 2024

projections that use GIA models that consider 3D Earth structure, which we refer to as 3D GIA models (van Calcar et al., 2024).

In the Amundsen Sea embayment, mantle viscosity can be as low as 10^{19} Pa·s (Barletta et al., 2018). Incorporating a low-viscosity zone in the upper mantle within a 1D GIA model leads to a significant stabilizing effect on the ice sheet over thousands of years (Pollard et al., 2017). However, using different relaxation times for East and West Antarctica did not contribute significantly to the uncertainty in the multi-centennial response of the Antarctic ice sheet to climate change. This can be explained by the chosen relaxation times for West Antarctica which were longer than 1000 years, while they might be a lot shorter in this region (Bulthuis et al., 2019). Other research has demonstrated that using a laterally varying relaxation time in the ELRA model (LVELRA) with a shorter relaxation time under West Antarctica results in a significantly reduced sea level contribution from Antarctica on multicentennial-to-millennial timescales for four different warming scenarios of 5000 years (Coulon et al., 2021). While it has long been possible to determine relaxation time spectra for radially varying viscosity profiles (McConnell, 1965), such calculations have not been performed for profiles with both lateral and radial variations in viscosity. Consequently, the variation in mantle relaxation times across Antarctica remains unknown.

A laterally varying relaxation time can be implemented in a straight-forward way in an ELRA model (Oude Egbrink, 2018; Coulon et al., 2021). However, sea level projections generated using coupled ELRA-ice sheet models have not been compared with the output from coupled ice sheet-3D GIA models, leaving it unclear how well different relaxation times and 1D mantle viscosity profiles are able to approximate the behaviour seen in more complex models that include 3D Earth structure. We used the ice sheet model IMAU-ICE coupled to ELRA and a GIA model to answer the following research questions:

1. How well can a coupled ice sheet – ELRA model using uniform relaxation time approximate the ice sheet evolution resulting from a coupled ice sheet - GIA model using a 3D Earth structure?
2. How well can a coupled ice sheet – ELRA model using laterally varying relaxation time approximate the ice sheet evolution resulting from a coupled ice sheet - GIA model using a 3D Earth structure?
3. How well can a coupled ice sheet – GIA model with a 1D Earth structure approximate the ice sheet evolution resulting from this model with a 3D Earth structure?

To address these questions, 3D GIA simulations are conducted using a global spherical finite element model coupled to the ice sheet model IMAU-ICE (van Calcar et al., 2024). We use constraints from seismic velocity studies to determine the spatially-varying rheological properties of the mantle (Wu et al., 2013). Output from models that employ 3D and 1D Earth structures, and maps of different relaxation times are compared in terms of sea level rise, grounding line position, ice thickness and bedrock uplift. As a result, we recommend values for uniform relaxation times in combination with the flexural rigidity that results in a sea level rise close to the average sea level rise resulting from two 3D Earth structures, one based on a viscosity constraint in the Amundsen Sea Embayment, and one based on a constraint in the Weddell Sea Embayment and Palmer land in the Antarctic Peninsula. Furthermore, we derive a relation between relaxation time and viscosity and recommend a laterally varying relaxation time map in combination with a flexural rigidity. Last, we recommend a 1D viscosity profile to approximate a 3D viscosity profile.

https://doi.org/10.5194/egusphere-2024-2982
Preprint. Discussion started: 30 October 2024

2 Method

To compare the performance of the ELRA, LVELRA and 1D GIA models with that of a 3D GIA model, we conduct sea level projections using the ice sheet model IMAU-ICE coupled to all three of these GIA models (van Calcar et al., 2024). We compare the Antarctic ice sheet evolution over the next 500 years under different warming scenarios and climate models using a variety of Earth structures. An overview of the simulations with different Earth models is provided in table 1. We use the low emission scenario SSP1.2-6 and the high emission scenario SSP5.8.5 and the climate models CESM, where warming mainly occurs in the Weddell sea, and IPSL, with warming mainly in the Amundsen Sea. The climate models provide ocean temperature, salinity and atmospheric temperature anomalies, and precipitation ratios until the year 2300, which are used to force the ice sheet model. The forcing is kept constant between 2300 and 2500.

The ice dynamical model IMAU-ICE is based on the shallow ice and shallow shelf approximations (Morland, 1985; Bueler & Brown, 2009; Berends et al., 2022). Ice velocities are computed on a 16 km grid resolution. Basal sliding follows the regularized Coulomb law (Zoet & Iverson, 2020). Basal melt at the ice shelf is computed using the Favier quadratic method and the surface mass balance is computed using a temperature and radiation parametrization (Favier et al., 2019; Berends et al., 2022). The present-day bedrock and ice surface topography are taken from Bedmachine version 3 (Morlighem et al., 2020).

Table 1: Different Earth structures used in the coupled ice sheet – Earth models. The 3D-stronger and Weaker structures are taken from van Calcar et al. (2024).

ELRA	1D GIA	3D GIA
Uniform (3000, 1500, 500, 400, 300, 200, 50 yr)	1D21	3D-stronger
2D-stronger	1D20	3D-weaker
2D-weaker	1D19	
	1D18	

2.1 1D and 3D GIA models

To compute the Earth's deformation, a global spherical finite element model based on Abaqus software is used. This model is used for two purposes: (1) To produce realistic sea level projections via coupling to the ice sheet model, and (2) to calculate the relaxation time of schematic ice unloading experiments which are used to derive a relation between relaxation time and viscosity.

In the GIA model, deformation in the upper mantle is assumed to be governed by diffusion and dislocation creep in olivine (Hirth & Kohlstedt, 2003) as in earlier studies (van der Wal et al., 2013; van der Wal et al., 2015; Blank et al., 2021, van Calcar et al., 2023; van Calcar et al., 2024). We do not specify lithospheric thickness, but instead use seismic velocity perturbations to assign appropriate rheological properties in each element between 35 and 670 km depth. At shallower depths, the layer is defined to be purely elastic. At deeper depths, the lower mantle is assumed to be homogenous. The effective viscosity, η_{eff}, is a function of the von Mises stress, q, and hence it is an output of the model rather than a property that is assumed *a priori*:

https://doi.org/10.5194/egusphere-2024-2982
Preprint. Discussion started: 30 October 2024

$$\eta_{\text{eff}} = \frac{1}{3B_{\text{diff}} + 3B_{\text{disl}} q^{n-1}} \quad (1)$$

Here, n is the stress exponent, and B_{diff} and B_{disl} are creep parameters for diffusion and dislocation creep as shown in Eq. 2a and 2b (Hirth and Kohlstedt, 2003).

$$\mathrm{B}_{diff} = \mathrm{A}_{diff} d^{-3} f_{H_2O}^{1} e^{-\frac{E+PV}{RT_{x,y}}} \quad (2a)$$

$$\mathrm{B}_{disl} = \mathrm{A}_{disl} d^{0} f_{H_2O}^{1.2} e^{-\frac{E+PV}{RT_{x,y}}} \quad (2b)$$

A is experimentally determined (A_{diff} = 10^6 MPa, A_{disl} = 90 MPa), d is the grain size, f_{H_2O} is the water content, E is the activation energy, P is the depth dependent pressure (Kearey et al., 2009), V is the activation volume, R is the gas constant and $T_{x,y}$ is the spatially variable absolute temperature. A, E and V are different according to the values for wet and dry olivine. All parameters, except temperature, grain size and water content, are taken from Hirth and Kohlstedt (2003). In this study, melt content is neglected as it has a relatively small influence on viscosity in this formulation (van der Wal et al., 2015). $T_{x,y}$ is the spatially varying mantle temperature, which is derived from a high resolution seismic model (Lloyd et al., 2019) in combination with a global seismic model from Becker and Boschi (2002). The mantle temperature variations are determined by converting these global seismic velocity perturbations to temperature perturbations using derivatives from Karato (2008), and then converting these to absolute temperature assuming a standard mantle geotherm (Turcotte and Schubert, 2002).

The upper mantle viscosity can vary greatly depending on the grain size and water content used. To obtain a realistic rheology, two different combinations of grain size and water content are chosen such that the average viscosity values across the Amundsen Sea Embayment and the Weddell Sea Embayment are the same as those constrained by GIA observations (Ivins et al., 2023), resulting in a relatively weaker 3D structure (labelled 3D-weaker) and a relatively stronger 3D Earth structure (labelled 3D-stronger) respectively (van Calcar et al., 2024). Since the viscosity is constrained by observations, both structures are considered realistic and not just an upper or lower limit. Background stress that contributes to the variable q in Eq. 1 is ignored here. Including background stress from the long-term GIA signal would lower viscosity, which will be compensated by grain size and water content parameters to still match the viscosity constraints.

For the coupling to the ice model, the GIA model is used with 9 vertical layers (0-35 km, 35-100 km, 100-150 km, 150-300 km, 300-420 km, 420-550 km, 550-670 km, 670-1171 km, and 1171-2890 km, and 2890-6371 km). Laterally varying B_{diff} and B_{disl} are assigned to each element between 35 and 670 km depth following Eq. 2a and 2b, respectively. The viscosity according to Eq. 1 determines if an element behaves effectively elastic; the lithosphere thickness is not specified explicitly. At shallower depths, the layer is defined to be purely elastic. At deeper depths, the lower mantle is assumed to be homogenous. A high resolution area is defined over Antarctica with a horizontal and vertical grid resolution of 35 km wide and deep between the surface and 670 km depth. The spatial resolution outside the high-resolution area is 200 km.

https://doi.org/10.5194/egusphere-2024-2982
Preprint. Discussion started: 30 October 2024

Different methods can be used to simulate the response due to 1D Earth structures (Peltier, 1974; Wu, 1998) but here we use the same GIA model to simulate 1D Earth structures and 3D Earth structures to avoid introducing differences that arise due to model formulation.

The relatively high computation time of the GIA model limits the number of cases we can investigate. Four 1D Earth structures are applied in the GIA model: one commonly used structure with an upper mantle viscosity of 10^{21} Pa·s, two structures with an upper mantle viscosity of 10^{20} and 10^{19} Pa·s, respectively, to represent the average viscosity under West Antarctica, and one with an upper mantle viscosity between $5{\cdot}10^{18}$ and $3{\cdot}10^{19}$ Pa·s that could represent the Amundsen Sea embayment (Barletta et al., 2018). These structures are hereafter referred to as 1D21, 1D20, 1D19 and 1DASE, respectively. Fig 1 shows the 1D viscosity variations with depth.

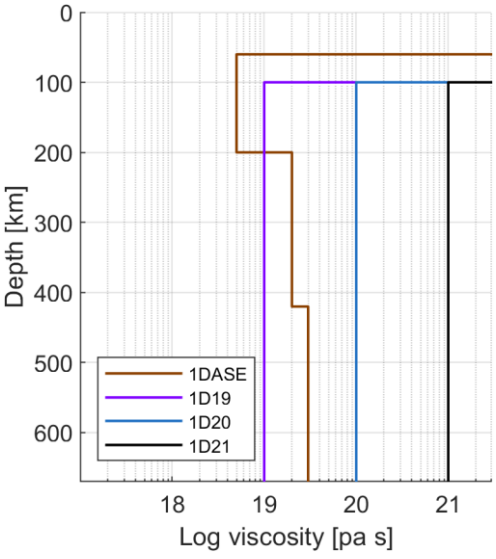

Figure 1: Upper mantle viscosity of the 1D Earth structures.

To derive a relation between relaxation time and viscosity, we used uplift rates from a schematic experiment using a 3D GIA model. In this case, the spatial resolution is 2 degrees at the surface and includes 8 vertical layers following van der Wal et al., 2013 and van der Wal et al., 2015 (0-35 km, 35-70 km, 70-120 km, 120-170 km, 170-230 km, 230-400 km, 400-670 km, and 670-2890 km), which we label as configuration 2, and the GIA model with variable resolution as 'configuration 1'. This resolution allowed us to run many schematic experiments. We used a global seismic model from Schaeffer & Lebedev (2013) combined with the regional seismic model of Heeszel et al. (2016) derived from Rayleigh wave array analysis over Antarctica to create a global seismic model. Uncertainties in the regional seismic model are used to ensure a smooth transition between values defined by the regional and global seismic models. The mantle temperature is then obtained following the same procedure as described for configuration 1. The dislocation and diffusion parameters are then computed using the mantle temperature, stresses, and a suite of globally-uniform values for grain size (1, 4, and 10 mm) and water content (0 or 1000 ppm H_2O). Below 400 km, uniform creep parameters are adopted, which yield mantle viscosities of ~10^{21}-10^{23} Pa s. The 3D GIA model is coupled to a code that solves the sea-level equation (Farrell & Clark, 1976) as implemented by Wang and Wu (2006).

2.2 ELRA

In ice sheet modelling, the Earth properties are often simplified to the ELRA approximation as described in detail in Le Meur & Huybrechts (1996). In this approach, bedrock deformation is dependent on a point load, the flexural rigidity and the relaxation time. The flexural rigidity (D) determines, together with the density of the asthenosphere and the gravity acceleration at the surface, the radius of relative stiffness (L_r) as shown in Eq. 3.

https://doi.org/10.5194/egusphere-2024-2982
Preprint. Discussion started: 30 October 2024

$$L_r = \left(\frac{D}{\rho_a g}\right)^{\frac{1}{4}} \quad (3)$$

First, the equilibrium deflection (w) at a normalized distance (x) from a point load (q) is computed using

$$w(x) = \frac{qL_r^2}{2\pi D} \cdot X(x), \quad (4)$$

where X is the zeroth order Kelvin function of x. The normalized distance is defined as the real distance (r) from the point load divided by the radius of relative stiffness. The total deflection at each point is the sum of the deflection at all neighboring points within a distance of six times the radius of relative stiffness.

Second, the bedrock deflection can be computed using

$$\frac{db(i,j)}{dt} = \frac{w(i,j) - b(i,j)}{\tau}, \quad (5)$$

where $\frac{db}{dt}$ is the bedrock elevation change over time, b the current bedrock elevation, τ the relaxation time and i, j the grid coordinates.

Besides the commonly used relaxation time of 3000 years and flexural rigidity of 10^{25} N·m, we also applied a relaxation time of 1500, 500, 450, 400, 350, 300, 250, 200 and 50 years in combination with a flexural rigidity of $1.92 \cdot 10^{24}$ N·m. The flexural rigidities roughly correspond to lithospheric thicknesses of 100 km and 60 km. This can be derived from the definition of flexural rigidity:

$$D = \frac{Eh^3}{12(1-\nu^2)}, \quad (6)$$

with the Young's modulus (E) set to 100 GPa and the Poisson's ratio (ν) set to 0.25. The lithospheric thickness is defined by h.

For the laterally varying ELRA model, we simply made the relaxation time a function of the 2D grid coordinates, as shown in Eq. 7.

$$\frac{db(i,j)}{dt} = \frac{w(i,j) - b(i,j)}{\tau(i,j)}, \quad (7)$$

A laterally varying flexural rigidity is also possible to implement but it is more complex (Coulon et al., 2021), and the effect on bedrock deformation is limited (Coulon et al, 2021; Zhao et al., 2017; Mitrovica et al., 2011). We therefore used uniform flexural rigidity values of $1.536 \cdot 10^{25}$, $1 \cdot 10^{25}$, $4.5511 \cdot 10^{24}$, and $1.92 \cdot 10^{24}$ N·m, corresponding roughly to lithospheric thicknesses of 120, 100, 80 and 60 km (Eq. 6), in agreement with estimates for lithospheric thickness across West and East Antarctica (Lloyd et al., 2019).

https://doi.org/10.5194/egusphere-2024-2982
Preprint. Discussion started: 30 October 2024

3 Relation between 3D viscosity and relaxation time

For a viscous half-space with uniform mantle viscosity, the relaxation time is equal to the Maxwell relaxation time that can be computed directly from the viscosity and shear modulus (e.g. Turcotte and Schubert, 2002). However, in a more realistic Earth structure, there is no longer a simple relation between Maxwell time and viscosity. In analytic GIA models based on the normal mode method (e.g. Wu & Peltier, 1982), each eigenmode has a characteristic relaxation time, but the complete response is controlled by a weighted combination of modes that depends on the spatial scale of the load and the properties of the lithosphere. This implies that the relaxation time depends on the size of the ice sheet and that a single relaxation time cannot be derived. Here, using the 3D GIA model in configuration 2, we determine relaxation times empirically by analysing the solid Earth deformation triggered by the removal of schematic surface loads. These surface loads are chosen to reflect large and small areas of ice mass change for different regions in West Antarctica, such that the resulting empirical relationship between mantle viscosity and relaxation time accounts for the different mantle conditions beneath the regions where the load changes are taking place. The shape of each surface load is controlled by the resolution of the 2-degree finite element mesh that is used in this configuration of the 3D GIA model (Fig. 2a). The uniform thickness of each load is taken to be 500 m. Each load is placed on the Earth until equilibrium is reached, and then instantaneously removed.

A total of 40 simulations are conducted, varying the grain size, water content and region of loading. For each simulation, the displacement over time for each surface load/Earth model combination is computed for multiple time steps. From the displacement curve, the uplift rate through time is calculated by time differentiation. The relaxation time is computed as half the time it takes for solid Earth rebound rates to decrease by $1/e^2$ following instantaneous unloading (Table 1 in Supplemental materials). Averaging over two relaxation times reflects more accurately the fact that viscosities at different depths will control the deformation at different stages of the relaxation.

Typically, depth averaged viscosities are computed by taking the average of the log of the viscosity values in a certain layer or area (e.g. Paulson et al., 2005; Whitehouse et al., 2006; Bagge et al., 2021). The filled symbols in Fig. 2b show the characteristic relaxation time of each region plotted against the average mantle viscosity, calculated as the volume-weighted mean viscosity of all elements between 120 and 400 km depth beneath each unloaded region indicated in Fig. 2a. However, the actual region of the mantle that predominantly influences the response depends on the sensitivity of the Earth to the specific loading, which depends on the viscosity profile itself (Peltier, 1976; Wu 2006). The sensitivity to the viscosity profile can be taken into account by computing the vertically averaged viscosities weighted by the local strain rate (Christensen, 1984). Such a procedure would result in average viscosity values that are determined more by low viscosity values in sub-surface Antarctica (because low viscosity regions will experience the highest strain rates). To take that into account, the computed relaxation times are compared to not only the average mantle viscosity value for each region, but also the lowest mantle viscosity derived from the seismic model, which is shown by the open symbols in Fig. 2b. A linear fit through the resulting log-log graph provides a relation between relaxation time in years, τ, and viscosity in Pa·s for the average viscosity (Eq. 8, solid line in Fig. 2) and the lower bound viscosity (Eq. 9, dashed line in Fig. 2).

https://doi.org/10.5194/egusphere-2024-2982
Preprint. Discussion started: 30 October 2024

$$\tau = 10^{\log(\eta_{\text{eff}})\cdot 0.35 - 4.63} \quad (8)$$

$$\tau = 10^{\log(\eta_{\text{eff}})\cdot 0.20 - 1.41} \quad (9)$$

Both relations will be used to create 2D relaxation time maps to identify which one is best approximating the sea level rise projections resulting from the coupled 3D GIA – ice sheet model. When the 2D relaxation time maps are used in an ELRA model, the relaxation time should be smoothly varying because otherwise discontinuities in deformation arise. Either a high-resolution viscosity profile should be used, because this will likely not contain large sharp changes in viscosity, or the relaxation time map should be smoothed.

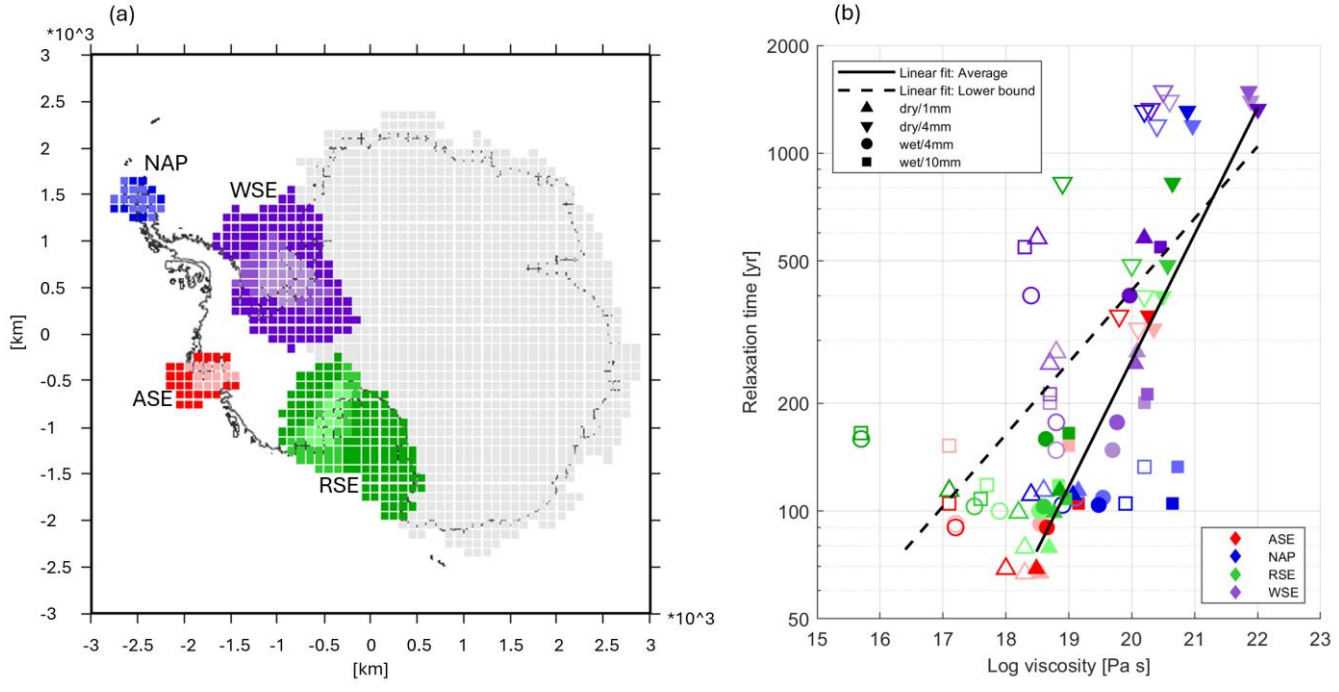

Figure 2: The relationship between mean upper mantle viscosity and relaxation time across West Antarctica. (a) Regions from which ice is instantaneously unloaded in order to determine regional relaxation times. Within each of the four main regions, there is a large and a small version of the region, coloured in dark and light colours respectively. The small region overlaps the large region. NAP refers to Northern Antarctic Peninsula, WSE refers to Weddell Sea Embayment, ASE refers to Amundsen Sea Embayment, and RSE refers to Ross Sea Embayment. (b) Log-log plot of relaxation time against mean upper mantle viscosity and the lower bound viscosity. The colours are identical to (a). The symbols reflect the parameters in the 3D GIA model used in each experiment (see Extended Data Table 1). The filled symbols reflect the average viscosity and the open symbols reflect the lower bound viscosity.

Using our empirically derived relationships between viscosity and relaxation time (Eq. 8, 9), we derive laterally variable relaxation time maps based on the 3D-weaker and 3D-stronger Earth models described in section 2.1. η_{eff} is taken to be the viscosity of the 3D Earth structure vertically averaged between 120 and 400 km depth (Fig. 3a,d). For the ice thickness changes in the projections of the ice sheet evolution by the ice sheet model, the highest sensitivity will be in this relatively shallow layer (Barletta et al., 2018). This results in two relaxation time maps based on the 3D-weaker rheology, hereafter referred to as 2D-weaker Average and 2D-weaker Lower bound (Fig. 3 b-c), and two relaxation time maps based on the 3D-stronger

https://doi.org/10.5194/egusphere-2024-2982
Preprint. Discussion started: 30 October 2024

rheology, hereafter referred to as 2D-stronger Average and 2D-stronger Lower bound (Fig. 3 e-f). Finally, the minimum relaxation time is set to 67 years, equal to the minimum relaxation time found in the experiments used to derive Eq. 8 and Eq. 9.

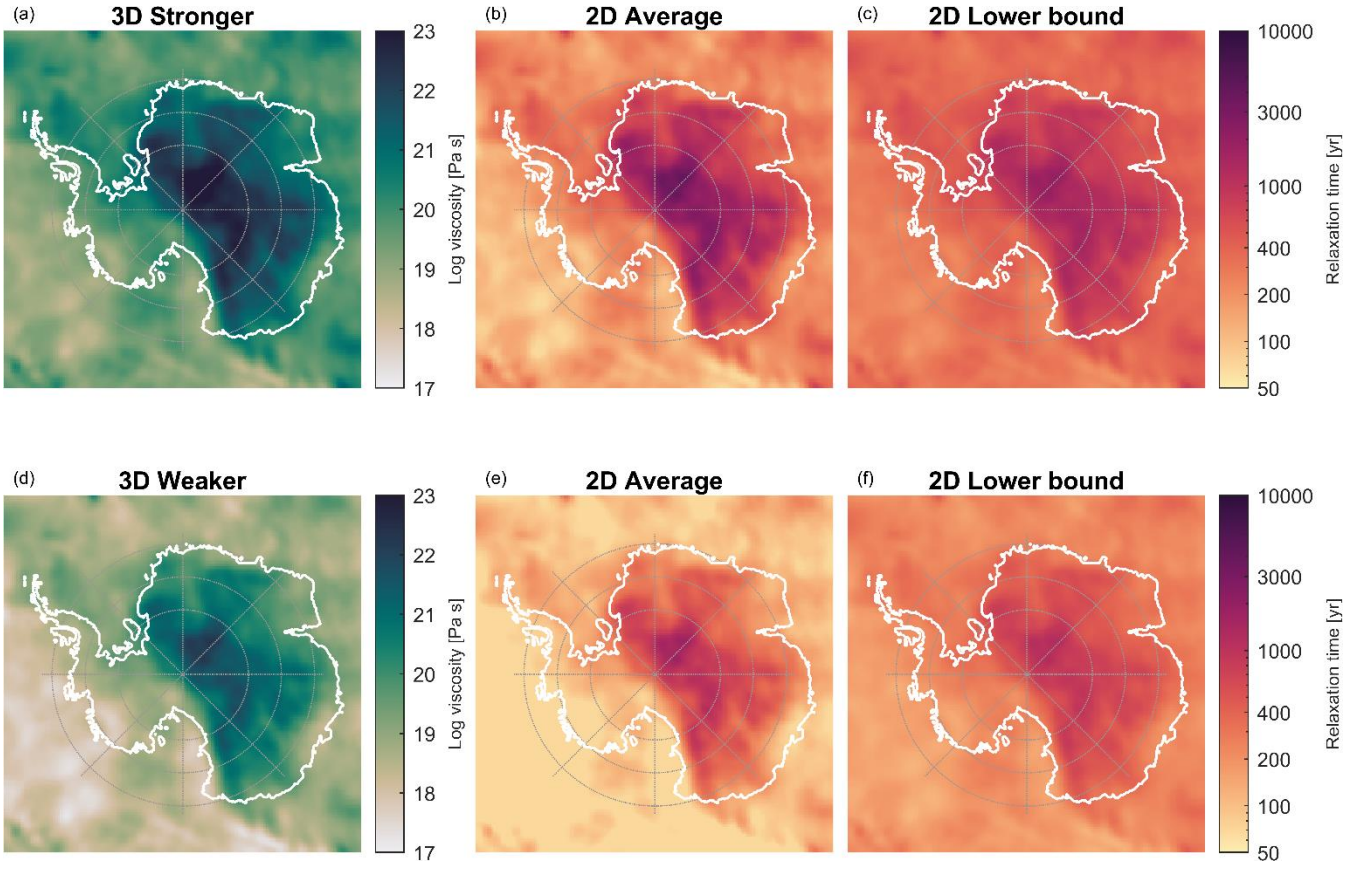

Figure 3: Panels a and d show the vertically averaged mantle viscosity between 120 and 400 km depth based on van Calcar et al. (2024). Panels b and e show the relaxation time maps computed using Eq. 8, and 3D-stronger and 3D-weaker, respectively. Panels c and f show the relaxation time maps computed using Eq. 9, and 3D-stronger and 3D-weaker, respectively.

4 Projections using different approaches to bedrock response

The sea level rise is projected for the coming 500 years using two different climate models for a high and a low emissions scenario. The sea level rise projected using simple models that adopt a uniform relaxation time, a laterally variable relaxation time and a 1D Earth structure is compared to the average sea level rise projected when using the 3D-weaker and 3D-stronger Earth structures within the GIA model in configuration 1. The average barystatic sea level rise computed by the ice sheet model using the two different 3D Earth structures is referred to as 3D-Average.

https://doi.org/10.5194/egusphere-2024-2982
Preprint. Discussion started: 30 October 2024

4.1 A uniform relaxation time

The bedrock response is dependent on the climate model because different regions of ocean warming cause different regions of ice retreat, and the mantle viscosity differs in each region. The bedrock response depends on the emission scenario as well, since a larger region of ice mass loss will trigger deformation deeper in the mantle where viscosity, and hence relaxation times, will be different to values at shallower depths (Peltier, 1976). The sea level rise resulting from the coupled ice sheet – GIA model using a 3D Earth structure therefore differs from a uniform relaxation time, and this difference in turn varies for different emission scenarios and climate models.

To assess the performance of the ELRA model with a uniform relaxation time, the resulting sea level rise is compared to the sea level rise averaged from the output of the two models that employ 3D Earth structures (3D-Average). The widely used uniform relaxation time of 3000 years (hereafter referred to as ELRA3000) overestimates the contribution from the AIS to sea level rise by 0.44-0.70 m (8-20%) in 2500 compared to the 3D-Average value, with the precise value depending on the emission scenario and the applied climate model (Fig. 4b,c,e,f). ELRA3000 overestimates sea level rise because this relaxation time is much longer than the relaxation time associated with the low viscosity values found in the 3D Earth structures (figure 3), especially when retreat occurs in the Amundsen Sea Embayment (as predicted by climate model IPSL) where the mantle viscosity is relatively low. We therefore search for a better choice of relaxation time, as formulated in research question 1: How well can a uniform relaxation time approximate the ice sheet evolution resulting from 3D Earth structures?

Out of the relaxation times investigated, we find that 300 years yields a reasonable approximation for the 3D results until year 2400, in combination with a flexural rigidity corresponding to 100 km lithospheric thickness (Fig. 4). For longer simulations, a 500 year relaxation time can be recommended. When a smaller lithospheric thickness of 60 km is applied, a longer relaxation should be considered (Supplemental Fig. 1). Since the combination of a higher flexural rigidity and shorter relaxation time yields a similar result to the combination of a lower flexural rigidity and somewhat higher relaxation time we only discuss the results for a flexural rigidity corresponding to a 100 km thick lithosphere in the following.

For the low emission scenario and by using the climate model IPSL, the difference in sea level rise between using a relaxation time of 300 yr (hereafter referred to as ELRA300) and 3D-stronger is negligible until 2400, but increases afterwards, reaching a maximum of 17 cm in 2500 (Fig. 4c), which is 5% of the total of 3.6 m of sea level rise using 3D-stronger (Fig. 4a). The ice is approximately 50 meter thicker within the Amundsen Sea Embayment using ELRA300 (Fig. 5a) due to faster uplift in this region compared to 3D-stronger. On timescales of 400 years and longer, it is not only the local low viscosity, but also the surrounding higher viscosities, which impact bedrock deformation in the 3D model. The rate of uplift predicted by the 3D GIA model therefore slows down on these longer timescales whereas the relaxation time in the ELRA model is constant over time and corresponds only to the low viscosities of the 3D model. As a consequence, the amount of bedrock uplift is about 75 m greater in ELRA300 than 3D-stronger between 2400 and 2500. The impact of the difference in bedrock elevation on ice mass loss and grounding line position is negligible. Contrary to this, the viscosity of 3D-weaker is much lower and the uplift predicted by ELRA300 is too slow compared to 3D-weaker over the full simulation time. The bedrock elevation of ELRA300

https://doi.org/10.5194/egusphere-2024-2982
Preprint. Discussion started: 30 October 2024

is tens of meters lower than 3D-weaker in 2300, causing faster retreat to be predicted by ELRA300 until 2500. In 2500, the grounding line has retreated about 150 km more in ELRA300 compared with 3D-weaker (Fig. 5).

For the high emission scenario, ELRA300 underestimates sea level rise by 0.4 m in 2500 compared with 3D-Average (Fig. 4a). When there is a larger region of ice mass loss, as is the case in the high emission scenario compared with the low emission scenario, the bedrock response is more sensitive to the rheology of deeper parts of the mantle, where the viscosity can be up to 3 orders of magnitude greater than at shallower depths. This causes the same effect as in the low emission scenario – a slowdown of the uplift projected by the 3D model on longer timescales – but the effect is even stronger. The relaxation time of ELRA300 is therefore too short compared to 3D-stronger and 3D-weaker on the long-term, leading to faster uplift and a higher bedrock elevation by 150 m in 2500 (Supplemental Fig. 2). However, around 2300, uplift in the 3D model has not slowed down much and is faster than the uplift of ELRA300. Therefore, at this moment in time, the ice is about 750 meters thicker in 3D-weaker compared with ELRA300 and the grounding line has retreated about 100 km less in the Amundsen Sea Embayment (Supplemental Fig. 3). The slowdown of bedrock uplift is less strong when retreat is concentrated in the Weddell Sea Embayment (using climate model CESM) due to less vertical variation in mantle viscosity in this region (Fig. 4e,f). To conclude, a relaxation time of 300 years fits best until 2400, but a relaxation time of 500 years should be chosen for longer simulations because of the increasing deviation of ELRA300 from 3D-Average over time.

https://doi.org/10.5194/egusphere-2024-2982
Preprint. Discussion started: 30 October 2024

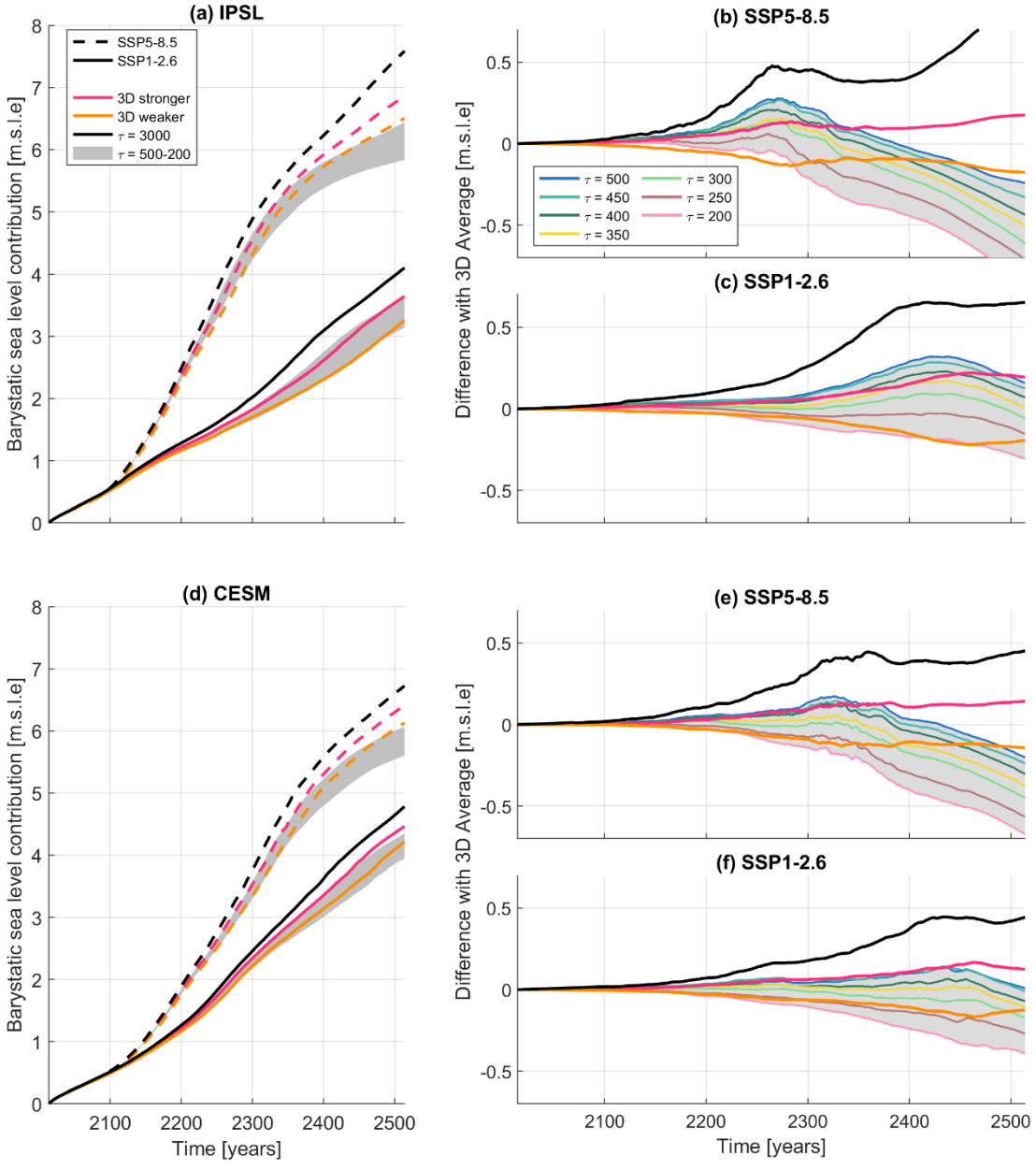

335

Figure 4. The Antarctic ice sheet contribution to barystatic sea level rise using the 3D GIA model and the ELRA model for a high and a low emission scenario and two different climate models, IPSL-CM6A-LR (panel a) and CESM2-WACCM (panel d). Two different Earth structures are applied in the 3D GIA model, a stronger Earth structure and a weaker Earth structure. The relaxation time of the ELRA model is varied between 200 and 500 years, and a reference run of 3000 years is used. The flexural rigidity of 10^{25} km·m^2 /s^2 roughly corresponds to a lithospheric thickness of 100 km. Panels b, c, e, and f show the difference in barystatic sea level contribution between the ELRA model with different relaxation times and the average sea level contribution of the two 3D GIA simulations.

340

https://doi.org/10.5194/egusphere-2024-2982
Preprint. Discussion started: 30 October 2024

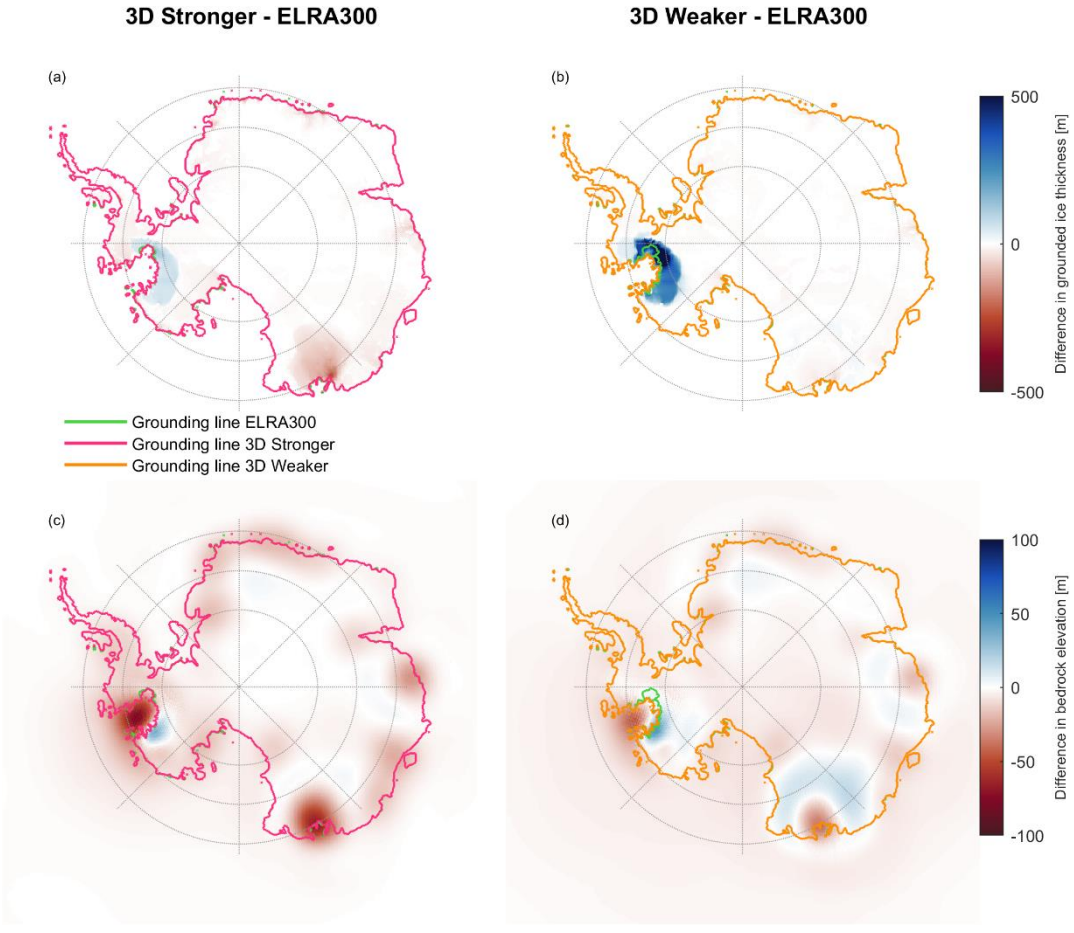

Figure 5: Difference in grounded ice thickness above flotation (panel a and b) and bedrock elevation (panel c and d) in 2500 between the ELRA model with a relaxation time of 300 years (referred to as ELRA300) and the two 3D Earth structures. Panels a and c correspond to 3D-stronger and panels b and d to 3D-weaker. The climate model IPSL is applied for the low emission scenario SSP1-2.6.

4.2 A laterally variable relaxation time

Previous studies have shown that a laterally varying Earth structure is needed to accurately simulate AIS evolution (Gomez et al., 2024; van Calcar et al., 2024). As these 3D GIA simulations are very costly, they prohibit large ensemble simulations. We therefore assess the performance of a 2D relaxation time, which is straight forward to implement in an ELRA model, to answer research question 2: How well can a laterally varying relaxation time approximate the ice sheet evolution resulting from 3D Earth structures?

We combined 4 different laterally varying relaxation time maps with different uniform flexural rigidities to investigate how well the computationally efficient ELRA model can replicate the results of the 3D models. As there is no *a priori* reason to select the average or lower bound viscosity equations, or a particular flexural rigidity, we investigate which of the resulting

https://doi.org/10.5194/egusphere-2024-2982
Preprint. Discussion started: 30 October 2024

ice sheet evolutions using the 2D maps correspond best to ice sheet evolution using the 3D-Average, and whether the improvement is significant compared to the performance of ELRA300. The different relaxation time maps, in combination with different lithospheric thicknesses, result in a large range of sea level rise projections. The 2D-stronger map, when combined with a flexural rigidity that corresponds to a lithospheric thickness of 120 km and derived from the average viscosity (Eq. 8), produces results which are closest to 3D-Average when considering both emissions scenarios and climate models (Fig. 8) and will be considered in the following. For the high emission scenario, the sea level rise is about 30-40 cm closer to 3D-Average at 2500 using 2D-stronger compared to using ELRA300 (Fig. 6a-b). The advantage of using 2D-stronger over ELRA300 is particularly great in the Amundsen Sea Embayment projections (IPSL) for scenarios longer than 400 years because the difference between 3D-Average and ELRA300 increases strongly after 2300, whereas the difference between 2D-stronger and 3D-Average is constant over time (Fig. 6a). In the high emission scenario driven by the IPSL climate model, the bedrock in the Amundsen Sea Embayment uplifted about 250 meters more by 2500 when using 2D-stronger compared with using the 3D GIA model (Supplemental Fig. 4). However, this uplift occurs mainly in the last 100 years and the effect on grounding line retreat is small due to the fact that the grounding line is already retreating rapidly and the West Antarctic ice sheet is in a phase of collapse.

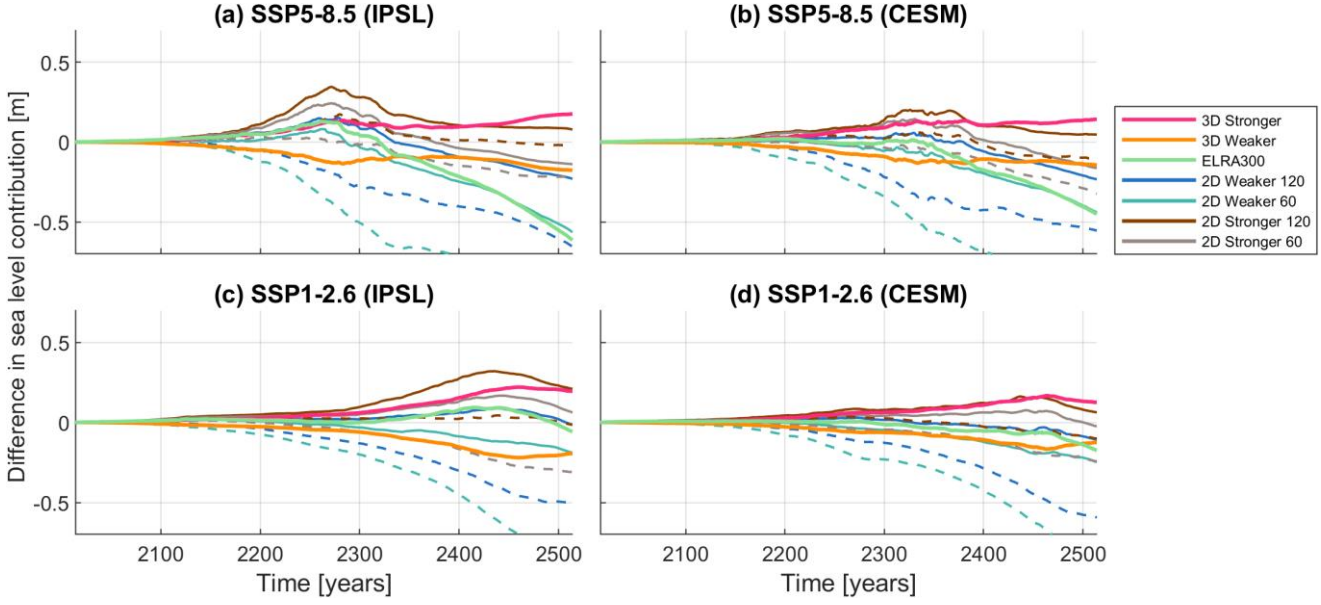

Figure 6: The difference in Antarctic ice sheet contribution to barystatic sea level rise between the average sea level contribution of the two 3D GIA simulations and the contribution using different 2D relaxation time maps. Results are shown for a high and a low emission scenario and two different climate models, IPSL-CM6A-LR and CESM2-WACCM. The dashed lines refer to the relaxation time calculated from the average viscosity (Eq. 8) and the solid lines refer to relaxation times calculated from the lower bound viscosity (Eq. 9). The numbers 120 and 60 in the legend refer to the lithospheric thickness.

https://doi.org/10.5194/egusphere-2024-2982
Preprint. Discussion started: 30 October 2024

4.3 1D GIA

Some ice sheet models are coupled with a 1D GIA model to conduct projections (Konrad et al., 2015; Whitehouse et al., 2019; Kachuck et al., 2020). The 1D GIA model is more realistic than the ELRA model because it takes into account the radial depth variation of viscosity, which implies a variable relaxation time as the size of the load determines which part of the radial viscosity profile controls the response. As 1D GIA models can also be considered intermediate in terms of computation time compared to ELRA and 3D GIA, we study whether 1D Earth structures offer an improved accuracy compared to ELRA models to answer research question 3: How well can a 1D Earth structure approximate the ice sheet evolution resulting from 3D Earth structures?

A widely used mantle viscosity for a 1D GIA model is 10^{21} Pa·s (hereafter referred to as 1D21) (Gomez et al., 2015; Konrad et al., 2015; Rodehacke et al., 2020; Golledge et al., 2019). Figure 7 shows that 1D21 overestimates the Antarctic sea level contribution by 0.4-0.55 m, depending on the emission scenario and climate model, because the structure is too stiff in West Antarctica compared to the 3D structures. The viscosity profiles 1DASE and 1D19 produce results similar to each other and to the 3D-Average model for the low emission scenario but, like ELRA300, they still underestimate the sea level contribution by 0.35 m in 2500 for the high emission scenario. The largest improvement of 1D19 compared to ELRA300 and 2D-stronger is in the bedrock uplift. The bedrock elevation of 1D19 in 2500 differs by a maximum of 80 meters from the results of the 3D GIA modelling in the high emission scenario, which is significantly smaller than the difference of 250 m when 2D-stronger is compared with the 3D GIA model output (Supplemental Fig. 5). To replicate not only the sea level contribution from 3D-Average, but also the geometry of the bed, it can therefore be recommended to use a 1D GIA model with an upper mantle viscosity of 10^{19} Pa·s instead of the ELRA model with a uniform relaxation time of 300 years or the 2D-stronger relaxation time map. Especially for long-term projections under a high emission scenario, the 1D GIA model is preferred over an ELRA model.

https://doi.org/10.5194/egusphere-2024-2982
Preprint. Discussion started: 30 October 2024

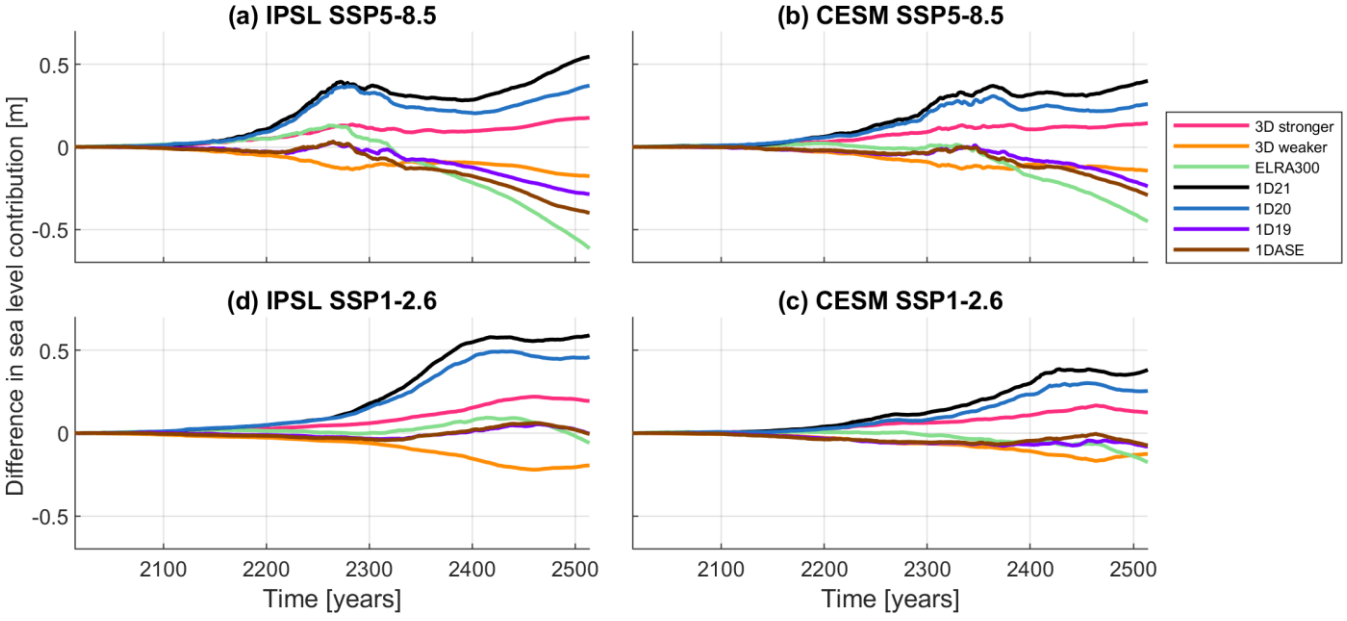

Figure 7: The difference in Antarctic ice sheet contribution to barystatic sea level rise between the average sea level contribution of the two 3D GIA simulations and the contribution using different 1D Earth structures. Results are shown for a high and a low emission scenario and two different climate models, IPSL-CM6A-LR and CESM2-WACCM. Note that the 1D19 and 1DASE mostly overlap for IPSL SSP1-2.6.

5. Conclusions and outlook

We investigated the accuracy of common implementations of bedrock adjustment within an ice model against ice model projections coupled to a GIA model with 3D variations in viscosity, for different emission scenarios and climate models. The ELRA model with a commonly used uniform relaxation time of 3000 years combined with a uniform flexural rigidity overestimates sea level rise by up to 0.70 m (20%) compared with the average barystatic sea level rise predicted using a model that includes 3D Earth structures. A 1D GIA model with an upper mantle viscosity of 10^{21} Pa·s overestimates sea level rise by up to 0.60 m (17%). To replicate the sea level rise of the average of the 3D GIA models (3D Average) better, a relaxation time or mantle viscosity corresponding to the area of ice mass loss should be chosen. We investigated the degree to which different bedrock models, Earth structures and parametrisations can replicate the bedrock uplift predicted by models that include 3D Earth structures.

Research question 1 was: How well can a uniform relaxation time approximate the ice sheet evolution resulting from 3D Earth structures? We recommend to use a uniform relaxation time of 300 years with a lithospheric thickness of 100 km to replicate the sea level rise predicted by a model that includes 3D Earth structure. Using this relaxation time results in a sea level rise that differs from 3D-Average by only 0.05-0.4 m, dependent on the emission scenario and the climate model. Note that using this relaxation time does lead to an increasing underestimation of sea level rise from 2400 onwards. Therefore, for simulations longer than 400 years, a relaxation time of 500 years is recommended. Even though the sea level rise can be similar between

https://doi.org/10.5194/egusphere-2024-2982
Preprint. Discussion started: 30 October 2024

ELRA300 and 3D-Average, the ice thickness can locally differ by up to 750 meters, the grounding position may differ by 100 km, and the bedrock elevation may differ by 150 meters between ELRA300 and the different 3D Earth structures. It is therefore recommended to vary the uniform relaxation time between 300 and 500 years to approximate the uncertainty from the 3D Earth structure.

With a small change in the ELRA model, a spatially varying relaxation time can be included. We derived an empirical relation between upper mantle viscosity and relaxation time and computed 2D maps of relaxation times to answer research question 2: How well can a laterally varying relaxation time approximate the ice sheet evolution resulting from 3D Earth structures? Applying the 2D-stronger map, derived using the relation between average viscosity for a strong 3D rheology and relaxation time, and a lithospheric thickness of 120 km, results in a sea level rise projection that differs from the 3D-Average value by only 10 cm in 2500. This difference doesn't increase on the long term in contrast to the ELRA model and it can thus be recommended to use ELRA with spatially varying relaxation time for long term simulations. Still, the bedrock elevation in 2D-stronger is hundreds of meters too high by 2500 compared to the 3D model under a high emission scenario.

For models that are able to use a 1D GIA model, we answer research question 3: How well can a 1D Earth structure approximate the ice sheet evolution resulting from 3D Earth structures? The use of an upper mantle viscosity of 10^{19} Pa·s results in sea level rise projections that only differ from 3D-Average by a maximum of 0.3 m. The bedrock elevation in 1D19 differs from 3D-Average by a maximum of 80 meters, thus this model provides the closest resemblance to the 3D Earth structures in terms of geometry, better than the ELRA and LVELRA models. However, the improvement should be traded off against a large increase in computation time. Our recommended values for the relaxation time and 1D viscosity will provide a better approximation of sea level rise than the currently used standard values but should be taken as guidelines and not as the true relaxation time or viscosity of the Earth's mantle. The simplified Earth models are all compared to the same coupled ice sheet - 3D GIA model and this model did not include the effect of a local sea level drop on ice sheet retreat. Including the feedback of the sea level drop on the ice sheet dynamics reduces the sea level rise by 5% compared to using a fixed sea level (van Calcar et al., 2024). Furthermore, different coupled ice sheet-3D GIA models could lead to different projections of sea level contribution, which might lead to somewhat different recommended values for relaxation time and 1D viscosity.

The laterally varying relaxation time is dependent on the 3D viscosity structure so different 2D relaxation time maps could be produced using the provided relation between relaxation time and viscosity. This allows other modellers to create their own relaxation time maps based on their preferred 3D viscosity profiles. If other regions and time periods are studied, these maps could be derived based on different seismic models, a different time period such as the deglaciation since the last glacial maximum, or for other regions such as Greenland.

https://doi.org/10.5194/egusphere-2024-2982
Preprint. Discussion started: 30 October 2024

Code and data availability

The supplemental data, i.e. Table 1 and the laterally varying relaxation time maps, are publicly available with doi 10.4121/a7215d4c-767f-49f1-a8bb-da40d0d2b01d**.** The data produced for this publication is available via doi 10.4121/b5548aaa-4c05-45f7-b0ce-775b83f13e5d. The source code of IMAU-ICE is included in this doi and can be found on Github: https://github.com/IMAU-paleo/IMAU-ICE. The GIA model code and coupling script has been made publicly available by van Calcar et al. (2023) with doi 10.4121/19765816.v2.

Author contributions

The conceptualisation was done by CvC, WvdW and RvdW. CvC, PW, and WvdW conducted model development and the experiments, and performed the data analysis with input from RvdW. All authors contributed to the writing of the manuscript.

Ethics declarations

There are no competing interests.

Acknowledgements

The authors would like to thank Ann Kristin Klose and Violaine Coulon for preparing and providing the forcing data of the climate models. We thank Matt King, Terry Wilson and Doug Wiens for discussions regarding the computation of relaxation times, and Dirk Oude Egbrink for his master thesis work which provided the first insights into the effect of a laterally varying relaxation time. Work for this publication was performed in the framework of PROTECT, which received funding from the European Union's Horizon 2020 Research and Innovation Programme under grant agreement No 869304. This is PROTECT publication number xxx (defined upon acceptance). The study was also supported by project 3D Earth funded by ESA as a Support to Science Element (STSE).

Additional information

Correspondence and requests for materials should be addressed to Caroline van Calcar (c.j.vancalcar@uu.nl).

References

Bagge, M., Klemann, V., Steinberger, B., Latinović, M., and Thomas, M.: Glacial-isostatic adjustment models using geodynamically constrained 3D Earth structures, Geochem. Geophys. Geosyst., 22(11), e2021GC009853, https://doi.org/10.1029/2021GC009853, 2021.

https://doi.org/10.5194/egusphere-2024-2982
Preprint. Discussion started: 30 October 2024

Barletta, V.R., Bevis, M., Smith, B., Wilson, T., Brown, A., Bordoni, A., Willis, M., Khan, S.A., Rovira-Navarro, M., Dalziel, I.W.D., Smalley, R., Kendrick, E., Konfal, S., Caccamise, D.J., Aster, R.C., Nyblade, A., and Wiens, D.A.: Observed rapid bedrock uplift in Amundsen Sea Embayment promotes ice-sheet stability, Science, 360, 1335–1339, https://doi.org/10.1126/science.aao1447, 2018.

Becker, T.W., and Boschi, L.: A comparison of tomographic and geodynamic mantle models, Geochem. Geophys. Geosyst., 3, https://doi.org/10.1029/2001GC000168, 2002.

Berends, C.J., Goelzer, H., Reerink., T.J., Stap., L.B., and van de Wal, R.S.W.: Benchmarking the vertically integrated ice-sheet model IMAU-ICE (version 2.0), Geosci. Model Dev., 15, 5667–5688, https://doi.org/10.5194/gmd-15-5667-2022, 2022.

Blank, B., Barletta, V., Hu, H., Pappa, F., and van der Wal, W.: Effect of lateral and stress-dependent viscosity variations on GIA induced uplift rates in the Amundsen Sea Embayment. *Geochemistry, Geophysics, Geosystems*, *22*(9), https://doi.org/10.1029/2021GC009807, 2021.

Book, C., Hoffman, M.J., Kachuck, S.B., Kachuck, S.B., Hillebrand, T.R., Price, S.F., Perego, M., and Bassis, J.N.: Stabilizing effect of bedrock uplift on retreat of Thwaites Glacier, Antarctica, at centennial timescales, Earth Planet. Sci. Lett., 597, 117798, https://doi.org/10.1016/j.epsl.2022.117798, 2022.

Bueler, E., and Brown, J.: Shallow shelf approximation as a “sliding law” in a thermomechanically coupled ice sheet model, J. Geophys. Res.-Earth, 114, F03008, https://doi.org/10.1029/2008JF001179, 2009.

Bulthuis, K., Arnst, M., Sun, S., and Pattyn, F.: Uncertainty quantification of the multi-centennial response of the Antarctic ice sheet to climate change, The Cryosphere, 13, 1349–1380, https://doi.org/10.5194/tc-13-1349-2019, 2019.

Coulon, V., Bulthuis, K., Whitehouse, P. L., Sun, S., Haubner, K., Zipf, L., and Pattyn, F.: Contrasting response of West and East Antarctic ice sheets to glacial isostatic adjustment, J. Geophys. Res.-Earth Surf., 126, e2020JF006003, https://doi.org/10.1029/2020JF006003, 2021.

Coulon, V., Klose, A., Kittel, C., Edwards, T., Turner, F., Winkelmann, R., and Pattyn, F.: Disentangling the drivers of future Antarctic ice loss with a historically calibrated ice-sheet model, The Cryosphere, 18, 653–681, https://doi.org/10.5194/tc-18-653-2024, 2024.

Christensen, U.: Convection with pressure- and temperature-dependent non-Newtonian rheology, Geophys. J. Int., 77, 343–384, https://doi.org/10.1111/j.1365-246X.1984.tb01939.x, 1984.

DeConto, R.M., Pollard, D., Alley, R.B., Velicogna, I., Gasson, E., Gomez, N., Sadai, S., Condron, A., Gilford, D.M., Ashe, E.L., Kopp, R.E., Li, D., and Dutton, A.: The Paris Climate Agreement and future sea-level rise from Antarctica, Nature, 593, 83–89, https://doi.org/10.1038/s41586-021-03427-0, 2021.

Farrell, W.E., and Clark, J.A.: On Postglacial Sea Level, Geophys. J. R. Astron. Soc., 46, 647–667, https://doi.org/10.1111/j.1365-246X.1976.tb01252.x, 1976.

https://doi.org/10.5194/egusphere-2024-2982
Preprint. Discussion started: 30 October 2024

Favier, L., Jourdain, N.C., Jenkins, A., Merino, N., Durand, G., Gagliardini, O., Gillet-Chaulet, F., and Mathiot, P.: Assessment of sub-shelf melting parameterisations using the ocean–ice-sheet coupled model NEMO(v3.6)–Elmer/Ice(v8.3), Geosci. Model Dev., 12, 2255–2283, https://doi.org/10.5194/gmd-12-2255-2019, 2019.

Fox-Kemper, B., Hewitt, H.T., Xiao, C.: Ocean, Cryosphere and Sea Level Change, in: Climate Change 2021: The Physical Science Basis. Contribution of Working Group I to the Sixth Assessment Report of the Intergovernmental Panel on Climate Change, Cambridge University Press, 1211–1362, https://doi.org/10.1017/9781009157896.011, 2021.

Golledge, N.R., Keller, E.D., Gomez, N., Naughten, K.A., Bernales, J., Trusel, L.D., and Edwards, T.L.: Global environmental consequences of twenty-first-century ice-sheet melt, Nature, 566, 65–72, https://doi.org/10.1038/s41586-019-0889-9, 2019.

Gomez, N., Pollard, D., and Holland, D.: Sea-level feedback lowers projections of future Antarctic Ice-Sheet mass loss, Nat. Commun., 6, 8798, https://doi.org/10.1038/ncomms9798, 2015.

Gomez, N., Yousefi, M., Pollard, D., DeConto, R. M., Sadai, S., Lloyd, A., Nyblade, A., Wiens, D.A., Aster, R.C., and Wilson, T.: The influence of realistic 3D mantle viscosity on Antarctica's contribution to future global sea levels, Sci. Adv., 10(31), eadn1470, https://doi.org/10.1126/sciadv.adn1470, 2024.

Heeszel, D.S., Wiens, D.A., Anandakrishnan, S., Aster, R.C., Dalziel, I.W.D., Hierta, A.D., Nyblade, A.A., Wilson, T.J., and Winberry, J.P.: Upper Mantle Structure of Central and West Antarctica from Array Analysis of Rayleigh Wave Phase Velocities, J. Geophys. Res.-Sol. Ea., 121, 1758–1775, https://doi.org/10.1002/2015JB012616, 2016.

Hirth, G., and Kohlstedt, D. L.: Rheology of the Upper Mantle and the Mantle Wedge: A View from the Experimentalists, in: Inside the Subduction Factory, edited by: Eiler, J., American Geophysical Union, Washington, D. C., USA, 83–105, https://doi.org/10.1029/138GM06, 2003.

Ivins, E. R., van der Wal, W., Wiens, D. A., Lloyd, A. J., and Caron, L.: Antarctic upper mantle rheology, in: The Geochemistry and Geophysics of the Antarctic Mantle, edited by: Martin, A. P. and van der Wal, W., https://doi-org.utrechtuniversity.idm.oclc.org/10.1144/M56-2020-19, 2023.

Jamieson, T.F. On the history of the last geological changes in Scotland. Quarterly Journal of the Geological Society, London, 21, 161–204, https://doi.org/10.1144/gsl.Jgs.1865.021.01-02.24, 1865.

Kachuck, S. B., Martin, D. F., Bassis, J. N., and Price, S. F.: Rapid viscoelastic deformation slows marine ice sheet instability at Pine Island Glacier, Geophys. Res. Lett., 47, e2019GL086446, https://doi.org/10.1029/2019GL086446, 2020.

Kaufmann, G., Wu, P., and Ivins, E. R.: Lateral viscosity variations beneath Antarctica and their implications on regional rebound motions and seismotectonics, J. Geodyn., 39(2), 165–181, https://doi.org/10.1016/j.jog.2004.08.009, 2005.

Konrad, H., Sasgen, I., Pollard, D., and Klemann, V..: Potential of the solid-Earth response for limiting long-term West Antarctic Ice Sheet retreat in a warming climate, Earth Planet. Sci. Lett., 432, 254–264, https://doi.org/10.1016/j.epsl.2015.10.008, 2015.

https://doi.org/10.5194/egusphere-2024-2982
Preprint. Discussion started: 30 October 2024

LeMeur, E., and Huybrechts, P.: A comparison of different ways of dealing with isostasy: examples from modelling the Antarctic ice sheet during the last glacial cycle, Ann. Glaciol., 23, 309–317, https://doi.org/10.3189/S0260305500013586, 1996.

Levermann, A., Winkelmann, R., Albrecht, T., Goelzer, H., Golledge, N. R., Greve, R., Huybrechts, P., Jordan, J., Leguy, G., Martin, D., Morlighem, M., Pattyn, F., Pollard, D., Quiquet, A., Rodehacke, C., Seroussi, H., Sutter, J., Zhang, T., Van Breedam, J., Calov, R., DeConto, R., Dumas, C., Garbe, J., Gudmundsson, G. H., Hoffman, M. J., Humbert, A., Kleiner, T., Lipscomb, W. H., Meinshausen, M., Ng, E., Nowicki, S. M. J., Perego, M., Price, S. F., Saito, F., Schlegel, N.-J., Sun, S. and van de Wal, R. S. W.: Projecting Antarctica's contribution to future sea-level rise from basal ice shelf melt using linear response functions of 16 ice sheet models (LARMIP-2), Earth Syst. Dynam., 11(1), 35–76, https://doi.org/10.5194/esd-11-35-2020, 2020.

Lloyd, A.J., Wiens, D.A., Zhu, H., Tromp, J., Nyblade, A.A., Aster, R.C., Hansen, S.E., Dalziel, I., Wilson, T., Ivins, E.R., and O'Donnell, J.P.: Seismic structure of the Antarctic upper mantle imaged with adjoint tomography, J. Geophys. Res.-Sol. Ea., 124, 1115–1130, https://doi.org/10.1029/2019JB017823, 2019.

McConnell, R.K.: Viscosity of the mantle from relaxation time spectra of isostatic adjustment, J. Geophys. Res., 70, 5171–5188, https://doi.org/10.1029/JZ070i020p05171, 1965.

Morland, L.W.: Unconfined ice-shelf flow, in: Dynamics of the West Antarctic Ice Sheet, edited by: Van der Veen, C. J., Oerlemans, J., D. Reidel Publishing Company, Dordrecht, the Netherlands, 99–116, https://doi.org/10.1007/978-94-009-3745-1, 1985.

Morlighem, M., Rignot, E., Binder, T. *et al.*: Deep glacial troughs and stabilizing ridges unveiled beneath the margins of the Antarctic ice sheet, Nat. Geosci., 13, 132–137, https://doi.org/10.1038/s41561-019-0510-8, 2020.

Mitrovica, J.X., Gomez, N., Morrow, E., Hay, C., Latychev, K., and Tamisiea, M.E.: On the robustness of predictions of sea level fingerprints, *Geophysical Journal International*, 187, 729–742, https://doi.org/10.1111/j.1365-246X.2011.05090.x, 2011.

Oude Egbrink, D.F.: Modelling the Last Glacial Ice Sheet on Antarctica with Laterally Varying Relaxation Time, MSc Thesis, Delft University of Technology, Delft, the Netherlands, 2018.

Paulson, A., Zhong, S., and Wahr, J.: Modelling post-glacial rebound with lateral viscosity variations, Geophys. J. Int., 163, 357–371, https://doi.org/10.1111/j.1365-246X.2005.02645.x, 2005.

Peltier, W. R.: The impulse response of a Maxwell Earth. *Reviews of Geophysics*, *12*(4), 649-669, https://doi.org/10.1029/RG012i004p0064, 1974.

Peltier, W.R.: Glacial-Isostatic Adjustment—II. The Inverse Problem, Geophys. J. Int., 46, 669–705, https://doi.org/10.1111/j.1365-246X.1976.tb01253.x, 1976.

Pollard, D., Gomez, N., and DeConto, R.M.: Variations of the Antarctic Ice Sheet in a coupled ice sheet-Earth-sea level model: Sensitivity to viscoelastic Earth properties, J. Geophys. Res.-Earth Surf., 122(11), 2124–2138, https://doi.org/10.1002/2017JF004371, 2017.

https://doi.org/10.5194/egusphere-2024-2982
Preprint. Discussion started: 30 October 2024

Ritsema, J., van Heijst, H.J., and Woodhouse, J.H.: Complex shear wave velocity structure imaged beneath Africa and Iceland, Geophys. J. Int., 184, 1223–1236, https://doi.org/10.1126/science.286.5446.1925, 2011.

Rodehacke, C.B., Pfeiffer, M., Semmler, T., Gurses, O., and Kleiner, T.: Future sea level contribution from Antarctica inferred from CMIP5 model forcing and its dependence on precipitation ansatz, Earth Syst. Dynam., 11(4), 1153–1194, https://doi.org/10.5194/esd-11-1153-2020, 2020.

Schaeffer, A.J., and Lebedev, S.: Global shear speed structure of the upper mantle and transition zone, Geophys. J. Int., 194, 417–449, https://doi.org/10.1093/gji/ggt095, 2013.

Seroussi, H., Nowicki, S., Payne, A.J., Goelzer, H., et al.: ISMIP6 Antarctica: a multi-model ensemble of the Antarctic ice sheet evolution over the 21st century, The Cryosphere Discuss., https://doi.org/10.5194/tc-2019-324, 2020.

Turcotte, D.L., and Schubert, G.: Geodynamics, 2nd edn., Cambridge University Press, Cambridge, United Kingdom, 2002.

van Calcar, C.J., van de Wal, R.S.W., Blank, B., de Boer, B., and van der Wal, W.: Simulation of a fully coupled 3D glacial isostatic adjustment – ice sheet model for the Antarctic ice sheet over a glacial cycle, Geosci. Model Dev., 16, 5473–5492, https://doi.org/10.5194/gmd-16-5473-2023, 2023.

van Calcar, C. J., Bernales, J., Berends, C.J., van de Wal, R.S.W., and van der Wal, W.: Assessing the interaction between ice dynamics, sub-shelf melt and GIA over a glacial cycle using a fully coupled GIA-ice sheet model. Preprint, 2024.

van Calcar, C. J., Bernales, J., Berends, C.J., van de Wal, R.S.W., and van der Wal, W.: Bedrock uplift reduces Antarctic sea-level contribution over next centuries. Preprint, https://doi.org/10.21203/rs.3.rs-4863941/v1, 2024.

van der Wal, W., Whitehouse, P. L., and Schrama, E. J. O.: Effect of GIA models with 3D composite mantle viscosity on GRACE mass balance estimates for Antarctica, Earth Planet. Sci. Lett., 414, 134–143, https://doi.org/10.1016/j.epsl.2015.01.001, 2015.

van der Wal, W., Barnhoorn, A., Stocchi, P., Gradmann, S., Wu, P., Drury, M., and Vermeersen, B.: Glacial isostatic adjustment model with composite 3-D Earth rheology for Fennoscandia, *Geophysical Journal International*, 194, 61–77, https://doi.org/10.1093/gji/ggt099, 2013.

Wang, H., and Wu, P.: Effects of lateral variations in lithospheric thickness and mantle viscosity on glacially induced relative sea levels and long wavelength gravity field in a spherical, self-gravitating Maxwell Earth, Earth Planet. Sci. Lett., 249(3–4), 368–383, https://doi.org/10.1016/j.epsl.2006.07.011, 2006.

Whitehouse, P., Gomez, N., King, M. A., and Wiens, D. A.: Solid Earth change and the evolution of the Antarctic Ice Sheet, Nat. Commun., 10, 503, https://doi.org/10.1038/s41467-018-08068-y, 2019.

Whitehouse, P. L., Latychev, K., Milne, G. A., Mitrovica, J. X., and Kendall, R.: Impact of 3-D Earth structure on Fennoscandian glacial isostatic adjustment: Implications for space-geodetic estimates of present-day crustal deformations, Geophys. Res. Lett., 33, L13502, https://doi.org/10.1029/2006GL026568, 2006.

Wu, P., and Peltier, W. R.: Viscous gravitational relaxation, Geophys. J. Int., 70, 435–485, https://doi.org/10.1111/j.1365-246X.1982.tb04976.x, 1982.

https://doi.org/10.5194/egusphere-2024-2982
Preprint. Discussion started: 30 October 2024

Wu, P. and Johnston, P.: Validity of Using Flat-Earth Finite Element Models in the Study of Postglacial Rebound, in: Dynamics of the Ice Age Earth, edited by: Wu, P., Trans Tech Publications Ltd, Switzerland, 191–202, 1998.

Wu, P.: Sensitivity of relative sea levels and crustal velocities in Laurentide to radial and lateral viscosity variations in the mantle, Geophys. J. Int., 165, 401–413, https://doi.org/10.1111/j.1365-246X.2006.02960.x, 2006.

Wu, P., and van der Wal, W.: Postglacial sealevels on a spherical, self-gravitating viscoelastic earth: Effects of lateral viscosity variations in the upper mantle on the inference of viscosity contrasts in the lower mantle, Geophys. J. Int., 192, 7–17, https://doi.org/10.1016/S0012-821X(03)00199-7, 2013.

Zhao, C., King, M. A., Watson, C. S., Barletta, V. R., Bordoni, A., Dell, M., and Whitehouse, P. L.: Rapid ice unloading in the Fleming Glacier region, southern Antarctic Peninsula, and its effect on bedrock uplift rates, Earth Planet. Sci. Lett., 473, 164–176, https://doi.org/10.1016/j.epsl.2017.06.002, 2017.

Zoet, L. K., and Iverson, N. R.: A slip law for glaciers on deformable beds, Science, 368(6486), 76–78, https://doi.org/10.1126/science.aaz1183, 2020.